J Mater Sci: Mater Med (2010) 21:489–496
DOI 10.1007/s10856-009-3931-x

A novel bioactive three-dimensional β-tricalcium phosphate/chitosan scaffold for periodontal tissue engineering

Feng Liao · Yangyang Chen · Zubing Li · Yining Wang · Bin Shi · Zhongcheng Gong · Xiangrong Cheng

Received: 25 August 2009 / Accepted: 1 November 2009 / Published online: 12 November 2009
© Springer Science+Business Media, LLC 2009

Abstract The development of suitable bioactive three-dimensional scaffold for the promotion of cellular proliferation and differentiation is critical in periodontal tissue engineering. In this study,porous β-tricalcium phosphate/chitosan composite scaffolds were prepared through a freeze-drying method. These scaffolds were evaluated by analysis of microscopic structure, porosity, and cytocompatibility. The gene expression of bone sialoprotein (BSP) and cementum attachment protein (CAP) was detected with RT-PCR after human periodontal ligament cells (HPLCs) were seeded in these scaffolds. Then cell–scaffold complexes were implanted subcutaneously into athymic mice. The protein expression of alkaline phosphatase (ALP) and osteopontin (OPN) was detected in vivo. Results indicated that composite scaffolds displayed a homogeneous three-dimensional microstructure; suitable pore size (120 μm) and high porosity (91.07%). The composite scaffold showed higher proliferation rate than the pure chitosan scaffold, and up-regulated the gene expression of BSP and CAP. In vivo, HPLCs in the composite scaffold not only proliferated but also recruited vascular tissue ingrowth. The protein expression of ALP and OPN was up-regulated in the composite scaffold. Therefore, it was suggested that the composite scaffold could promote the differentiation of HPLCs towards osteoblast and cementoblast phenotypes.

Feng Liao and Yangyang Chen both authors have contributed equally to the work.

F. Liao · Z. Li · Y. Wang · B. Shi · Z. Gong · X. Cheng
Key Laboratory for Oral Biomedical Engineering of Ministry of Education, School and Hospital of Stomatology, Wuhan University, Wuhan 430079, People's Republic of China

Y. Chen
Department of Oncology, Tongji Hospital, Huazhong University of Science and Technology, Wuhan 430030, People's Republic of China

X. Cheng (✉)
Department of Prosthodontics, School and Hospital of Stomatology, Wuhan University, Wuhan, People's Republic of China
e-mail: lfcyy@163.com

1 Introduction

Periodontitis is an inflammatory disease invading the periodontium including gingival, periodontal ligament, cementum and alveolar bone, which could affect approximately 10% of adult population and lead to bone resorption and ultimately tooth loss [1]. The final goal of periodontal therapy is to restore the structure and function of the periodontium destroyed because of periodontitis. So far, various procedures have been proposed [2], including guided tissue regeneration, application of enamel matrix derivative, bone substitutes and autogenous bone grafting techniques. However, attempts at regeneration of periodontium by these methods have not always yielded predictable results [3]. The key limitation is the true regeneration of cementum, alveolar bone, and periodontal ligament anchored between them. Progress in tissue engineering has opened the world of regeneration of various tissues and organs. Recently, researchers have focused on the regeneration of periodontium using tissue engineering [4]. This approach consists of an interactive triad of responsive cells, supportive matrix (scaffold), and bioactive molecules promoting differentiation and regeneration.

The scaffold, which is used to create the three-dimensional organization needed for appropriate cell interactions, to serve as vehicles to deliver and retain the cells at a specific site, is a key element in tissue engineering. It

provides a three-dimensional porous and fully inter-penetrable space for tissue ingrowth, accelerates the formation of tissue structure, and ultimately is replaced by a new extracellular matrix (ECM) to form completely natural tissue [5]. Today, two important categories of materials are used for scaffolds. The first category of materials is natural or synthetic polymers such as polysaccharides, hydrogels or thermoplastic elastomers; the second category of materials is bioactive ceramics such as calcium phosphates and bioactive glasses or glass–ceramics. Chitosan is a deacetylated derivative of chitin, and it has been proved biologically renewable, biodegradable, biocompatible, non-antigenic, non-toxic, and bio-functional [6]. Chitosan possesses excellent ability to form porous structures and the applications of porous chitosan scaffolds for tissue engineering have been reported [7]. However, pure chitosan scaffold lacks bioactivity to induce hard tissue formation, which limits its application in tissue engineering.

Calcium phosphates are excellent candidates for bone tissue engineering because of their close chemical and crystal resemblance to bone mineral. They not only have an excellent biocompatibility, but also possess osteoconductive properties and may bind directly to bone under certain conditions [8]. Calcium phosphates have been reported to have good bioactivity, and the osteoblasts can readily form mineral deposits on the surfaces of calcium phosphates in vitro and in vivo [9]. Numerous in vivo and in vitro assessments have reported that calcium phosphates, no matter of which form (bulk, coating, powder, or porous) and of which phase (crystalline or amorphous), always support the attachment, differentiation, and proliferation of relevant cells (such as osteoblasts and mesenchymal cells) [10].

Currently, composites of polymers and bioactive ceramics are being developed with the aim to increase the mechanical scaffold stability and to improve tissue interaction [11]. The periodontal tissue is a composite structure including soft tissues (periodontal ligament and gingival) and hard tissues (alveolar bone and cementum). Therefore, composite systems combining advantages of polymers and ceramics seem to be a promising choice for periodontal tissue engineering. It is desirable to develop a composite material with favorable material properties of chitosan and calcium phosphates for periodontal regeneration.

Therefore, in this study, β-tricalcium phosphate (β-TCP)/chitosan composite scaffolds were constructed by a freeze-drying method and evaluated by analysis of microscopic structure and porosity. Then, the cytocompatibility was evaluated through seeding human periodontal ligament cells (HPLCs) into scaffolds in vitro. The morphology and distribution of HPLCs in these scaffolds were examined by confocal laser scanning microscope. The gene expression of bone sialoprotein (BSP), suggesting the initiation of bone mineralization, and cementum attachment protein (CAP), a marker molecule for cementogenesis, was detected with RT-PCR. Besides, HPLCs combined with scaffolds were implanted subcutaneously into athymic mice to evaluate the biocompatibility. In addition, the protein expression of alkaline phosphatase (ALP) and osteopontin (OPN), two important molecules involved in the formation of bone and cementum, was detected with modified Gomori's ALP staining [12] and immunohistochemical staining, respectively in vivo.

2 Materials and methods

2.1 Materials

Chitosan (minimum deacetylation degree of 85%) was obtained from Sigma (St. Louis, MO, USA). β-TCP was purchased from Sigma–Aldrich Com. Dulbecco's modified Eagle's medium (DMEM) and fetal bovine serum (FBS) were from Gibco Company. All other reagents were of analytical grade.

2.2 Fabrication of porous β-TCP/chitosan scaffolds

The chitosan was dissolved in a 2% acetic acid solution. Then, β-TCP powders were added to the solution. The mass ratio of β-TCP and chitosan in the mixture was 3:7 and the total concentration of β-TCP and chitosan was 1% (w/v). The solution was stirred for 48 h at 4°C. Then, this mixture was rapidly transferred to a freezer at −35°C overnight to solidify the solvent and induce solid–liquid phase separation. Then the solidified mixture was maintained at −80°C for 2 h and was transferred into a freeze-drying vessel (OHRIST BETA 1-15, Germany) for 48 h until dried. The scaffolds were soaked in 0.3 M NaOH, followed by washing with double-distilled water and immersed in 75% ethanol solution for 12 h for sterilization, and then lyophilized again to get neutral, asepsis scaffolds. Pure chitosan scaffold prepared by the same method was served as the control. The porosity of the scaffolds was determined by the liquid displacement method [13].

Scaffolds were divided into two groups: group 1, the pure chitosan scaffold group; group 2, the β-TCP/chitosan scaffold group.

2.3 Scanning electron microscopy (SEM) examination

The porous morphologies of the scaffolds were studied by SEM (Quanta 200). The groups 1 and 2 scaffolds were sectioned at various planes, sputter-coated with gold and observed by SEM. Mean pore diameters were determined by image analysis of digital SEM photo of sectioned samples.

2.4 HPLCs cultured into the scaffolds

HPLCs were obtained as previously described by Somerman et al. [14]. These HPLCs were used at passage 2–4 in experiments. After 90% confluence, cells were digested by 0.25% trypsin and cell density was adjusted to 1×10^7/ml. The sterilized scaffolds were shaped into $5 \times 5 \times 1$ mm pieces and transferred into 24-well plastic culture plates. After prewetted with culture medium overnight, 100 μl cell suspensions containing 10^6 cells were seeded into each scaffold. After 3 h, another 900 μl culture medium was supplied, and the culture was set at 37°C in 5% CO_2 humidified atmosphere.

2.5 Confocal laser scanning microscope (CLSM) observation

10^6 HPLCs were seeded into each scaffold in 24-well plastic culture plates. Two days after initial seeding, fluorescein diacetate (FDA, AnaSpec, Inc) solutions (5 mg/ml) were dropped into the cultured cells (3 μl/well). After incubated for 15 min at 37°C, the cell-scaffold complexes were examined with a confocal laser scanning microscope (CLSM, Leica, DMIRZ, Germany).

2.6 MTT assay

Scaffolds were transferred into 96-well plastic culture plates. 10^5 HPLCs were seeded into each scaffold ($n = 6$). The cells were allowed to adhere to the scaffolds for 3 h, and then the cell–scaffold complexes were covered with 150 μl of medium. The percentage of viable cells was determined every day after incubation. One hundred microliters of sterile MTT (5 mg/ml) was added to each well and incubated for 3.5 h at 37°C. At the end of incubation, the MTT solution was carefully aspirated without disturbing the pellets, and the resulting blue formazan product was solubilized in 200 μl of DMSO. The optical density values were determined at least in triplicate against a reagent blank at a test wavelength of 570 nm and reference wavelength of 630 nm. The values reflect the viable cell population in each well.

2.7 Reverse transcription-polymerase chain reaction (RT-PCR)

10^6 cells were seeded into each scaffold in 24-well plastic culture plates. Expression of BSP and CAP was confirmed by RT-PCR, 72 and 144 h after initial seeding. The total cell RNA was prepared from each scaffold ($n = 3$) harvested at 72 and 144 h by the TaKaRa kit (TaKaRa, Japan). Total RNA (1.0 μg) was used as template for the synthesis of cDNA with OligodT and AMV reverse transcriptase (TaKaRa, Japan). The following PCR amplification reaction used Taq polymerase and specific primers. The primers for the BSP gene (GenBank Accession No. NM_004967.2) were 5′-GCCTGTGCTTTCTCAATG-3′ and 5′-TTCCTTCCTC TTCCTCCTC-3′. The primers for the CAP gene (GenBank Accession No. NM_014241.3) were 5′-TGGCTCAC CTTCTACGACA-3′ and 5′-CCAGCAACTCCAACAGG AT-3′. The PCR products were visualized on a 1% (w/v) agarose gel by staining with ethidium bromide and analyzed densitometrically using Gel image software. The relative levels of mRNA expression were quantified by comparison with the internal control (β-actin). Each PCR was duplicated with the same total RNA.

2.8 In vivo study

Two kinds of scaffolds were located into 24-well culture plates and 10^6 HPLCs were seeded into each scaffold. Two days after initial seeding, the group 2 scaffolds were implanted into the left dorsal subcutaneous area of 12 athymic mice (BALB/c-nu;Hubei Medical Laboratory Animal Center). The group 1 scaffolds were implanted into right dorsal subcutaneous area as control. All animal experimental procedures were carried out under Guidelines and Regulations for the Use and Care of Animals of the Review Board of Hubei Medical Laboratory Animal Center.

The transplants were harvested at 4 weeks post-transplantation, the specimens were fixed in 4% paraformaldehyde for 24 h, decalcified in 10% EDTA for 48 h, dehydrated, embedded in paraffin, and sectioned serially at a thickness of 5 μm. The specimens were stained with hematoxylin and eosin (H&E), or used for immunohistochemical and modified Gomori's ALP staining. Primary antibodies against human osteopontin (OPN, Santa Cruz, CA) were used. Specimens were examined with light microscope.

2.9 Statistical analysis

All experiments were performed three times, with each treatment conducted in triplicate. Means and standard deviations (SD) were calculated, and the statistical significance of differences among each group was examined by Student's t-test and P values less than 0.05 were considered significant.

3 Results

3.1 The characterization of porous scaffolds

As shown in Fig. 1a, b, both pure chitosan and composite scaffolds showed open macroporous microstructure with a high degree of interconnectivity. The mean pore size of pure chitosan scaffold and composite scaffold was 160 μm

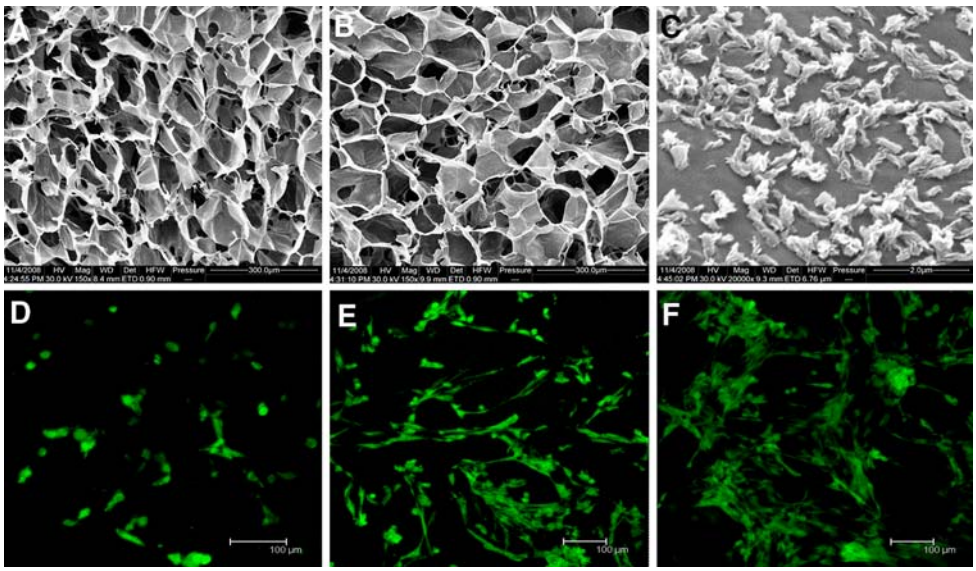

Fig. 1 SEM photographs of scaffold surface. Pure chitosan scaffold (**a**), β-TCP/chitosan composite scaffold (**b**), and the particle-like structures on the pores wall of β-TCP/chitosan composite scaffold (**c**). CLSM photographs of HPLCs after 2 days culture in vitro. Pure chitosan scaffold (**d**), β-TCP/chitosan composite scaffold (**e**), and complex three-dimensional network-like cell clusters formed by HPLCs in β-TCP/chitosan composite scaffold (**f**)

and 120 μm, respectively. Compared with the pure chitosan scaffolds, the composite scaffolds showed more regular pore structure and more homogeneous pore size. The surface of the pores wall was smooth and homogeneous in the pure chitosan scaffold, while some particle-like structures appeared on the pores wall of composite scaffold (Fig. 1c). It suggested the β-TCP particles spread in the chitosan matrix of the composite, combined with chitosan, and showed particle-like structure. The porosity of the pure chitosan scaffold and the composite scaffold was 90.90% and 91.07%, respectively.

3.2 CLSM observations

Morphology and distribution of viable HPLCs in the two kinds of scaffolds were observed by CLSM. On composite scaffold, live HPLCs (stained green) spread on the surface uniformly. Cells adapted closely to the surface and displayed flattened morphology (Fig. 1e). Cell–cell junction was also observed in every case. Two days after seeding, HPLCs not only spread on the surface of the scaffold, but also migrated into the inner space (120 μm in depth) to form complex three-dimensional network-like cell clusters (Fig. 1f). For the composite scaffolds, the HPLCs showed higher cell densities and more abundant cytoplasm. In contrast, the HPLCs in pure chitosan scaffolds showed scattered distribution and little cytoplasm (Fig. 1d).

3.3 Cell proliferation and viability

MTT assay was adopted to evaluate the cytotoxicity of the tissue engineering materials. The absorbencies of HPLCs in the scaffolds were shown in Fig. 2. It showed the percent of viable cells on group 2 scaffolds was significantly higher

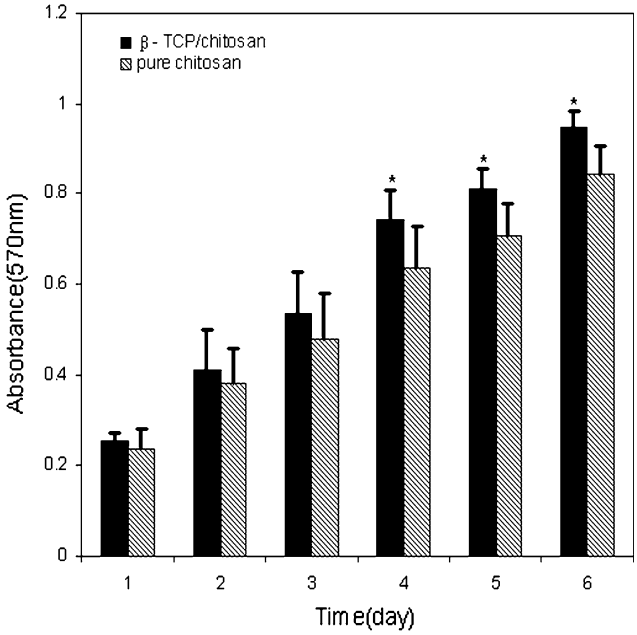

Fig. 2 The proliferation of HPLCs in two kinds of scaffolds was measured by MTT assay. The data showed the percent of viable cells on group 2 scaffolds was significantly higher than that on group 1 scaffold during the culture period (* $P < 0.05$)

than control scaffold during the culture period ($P < 0.05$), which suggested the HPLCs showed much better proliferation properties on group 2 than on group 1.

3.4 RT-PCR

RT-PCR showed that HPLCs altered their genetic expression during the culture periods (Fig. 3). RT-PCR analysis revealed the expected 439 bp BSP and 425 bp CAP DNA band, β-actin being an internal control. The significant

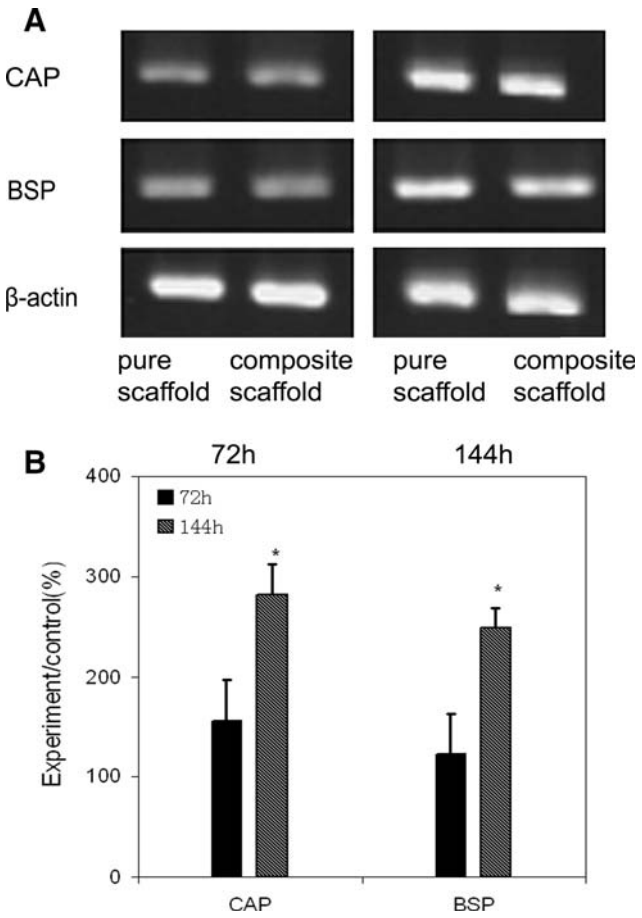

Fig. 3 RT-PCR analysis revealed the expected 439 bp BSP and 425 bp CAP DNA band, β-actin being an internal control. The significant differences were noted in the mRNA expression levels of BSP and CAP when the HPLCs were cultured in group 2 scaffolds (* $P < 0.01$)

differences were observed in the mRNA expression levels of BSP and CAP when the HPLCs were cultured in group 2 scaffolds ($P < 0.01$). The mRNA expression levels of BSP and CAP both increased in 72 and 144 h, and the increasing level of 144 h was greater than that of 72 h.

3.5 In vivo study

To investigate the biocompatibility of the composite scaffolds and the pure chitosan scaffolds in vivo, the athymic mice model was adopted. The HPLCs were seeded onto the scaffold using a static seeding method to verify that they could adhere to these scaffolds. All 12 animals survived from the experiment. There were no inflammatory reactions, infections, or extrusions. After 4 weeks' transplantation, two kinds of transplants could be clearly seen subcutaneously on the animals' dorsal area and kept the initial shape.

HE staining showed that many proliferated cells and abundant regenerated ECM filled the voids of the composite scaffolds. Vascular tissue ingrowth was noticed in the composite scaffolds (Fig. 4b). In contrast, the cells distributed sparsely and little ECM presented in the pure chitosan scaffolds (Fig. 4a). In both scaffolds, a few slivers of the degrading scaffolds distributed among the cells and ECM.

Immunohistochemical staining with antibody to OPN showed that only group 2 was stained after 4 weeks' transplantation (Fig. 4c, d).

ALP staining showed that positive black areas were only stained in group 2 (Fig. 4e, f).

4 Discussion

Tissue engineering strategies use combination of cells, biodegradable scaffolds, and bioactive molecules to recapitulate natural processes of tissue regeneration and development. The major parameter in tissue engineering is the choice of a suitable scaffold that plays a key role in seeding the cells and serves as a template for tissue regeneration. The design of a scaffolding material can significantly affect the cell seeding and growth both in vitro and in vivo [15]. Scaffolding materials should be biocompatible, biodegradable, and bioactive to let specific cells attach, proliferate, migrate, and differentiate on them. Chitosan satisfies many of these requirements. However, chitosan is nonbioactive but only biotolerable, which limits its application in tissue engineering. Calcium phosphates have been proven bioactive and osteoconductive, which is good to form hard tissue such as bone and cementum. For example, calcium phosphate ceramics such as hydroxapatite are widely utilized as bone graft substitutes [16]. They have bone-bonding properties that allow them to establish chemical bonds between the regenerated bone tissue and the surfaces of implants when they are implanted into bone defects. On the other hand, the key limitation in periodontal therapy is the true regeneration of cementum, alveolar bone, and periodontal ligament. Therefore, it is desirable to develop a composite material with favorable material properties of chitosan and calcium phosphates for the regeneration of the periodontal tissue. In the present study, we constructed β-TCP/chitosan composite scaffolds and evaluated β-TCP/chitosan materials as prospective candidates for periodontal tissue engineering. The composite scaffolds were prepared through a solid–liquid phase separation of the polymer solution and subsequent sublimation of the solvent. This is a low-cost and bioclean method for formulating biodegradable scaffolds without the use of any additives or organic solvents. The composite scaffold showed a homogeneous three-dimensional microstructure; suitable pore size and high porosity. It was reported the scaffold mean pore size significantly influenced cell

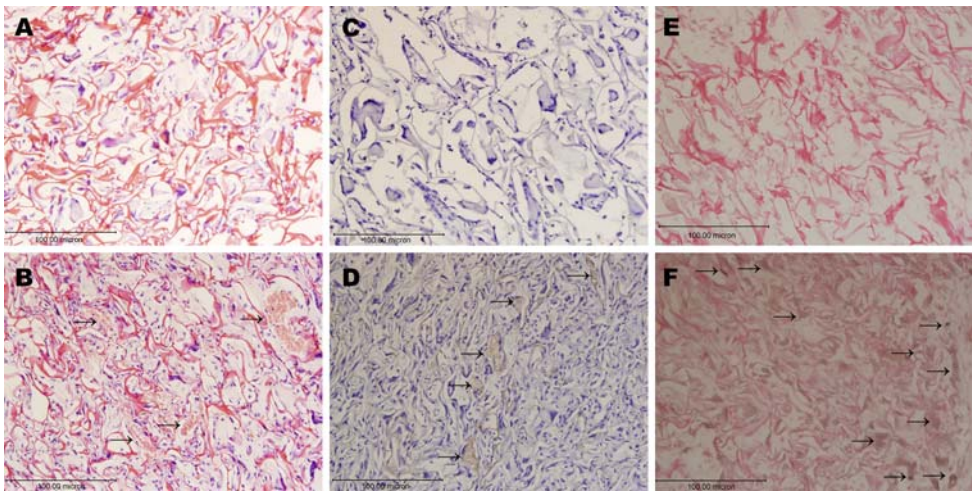

Fig. 4 Light micrographs of implants excised at 4 weeks after implantation. The cross-section was stained with hematoxylin and eosin. Cells distributed sparsely and little extracellular matrix presented in the pure chitosan scaffolds (**a**), and numerous proliferated cells and abundant regenerated extracellular matrix filled the voids of the composite scaffolds. The arrows indicated vascular tissue ingrowth (**b**). The cross-section was immunohistochemically stained with OPN antibody. Group 1 was negative (**c**), and the OPN was positively stained in group 2. The arrows indicated the positive areas (**d**). The cross-section was stained with modified Gomori's ALP stain. Group 1 was negative (**e**), and group 2 was positively stained. The arrows indicated the positive areas (**f**)

morphology and phenotypic expression [17]. Fibroblasts bound to a wide range of pore size from 63 to 150 μm and cells increased their viability with decreasing pore size until no cells could fit into the pores [18]. The pore size of the composite scaffold is 120 μm, which is favorable for the attachment and ingrowth of HPLCs. The scaffold with high porosity (higher than 90%) can not only provide large internal surface for cell adhesion and migration but also contribute to the exchange of nutrients and metabolic waste. Further, it can easily be made into the required shape and size. After two days' incubation, seeded HPLCs not only spread on the surface but also migrated into the inner space of the scaffold (120 μm in depth). In vivo study, histological examination showed the scaffolds were covered and filled with new tissue. The HPLCs produced exracellular matrices to fill the voids in the scaffold. The microsponges formed in the openings of composite scaffold provided abundant surface area for HPLCs attachment. In tissue engineering, scaffolds need to be designed to support the proper formation of vascular tissue and possess the mechanical properties that can match those of native arteries [19]. The results from the in vivo study showed that new vascular tissue had grown into the scaffold residues after 4 weeks implantation, which was important for the regeneration of periodontal tissue.

Periodontal ligament (PDL) is a soft connective tissue embedded between cementum and alveolar bone, to sustain teeth within the jaw. PDL contains heterogeneous cell populations,which have many osteoblast-like properties such as high levels of ALP and the ability to produce bone-associated protein [14]. Currently, PDL tissue is considered to contain pluripotent mesenchymal stem cells that can differentiate into cementum-forming cells, osteoblast-like cells, and connective tissue fibroblasts. Successful healing, repair, or regeneration of damaged periodontal tissue requires orchestration of cellular migration, proliferation, and differentiation of pluripotent mesenchymal stem cells in PDL [20]. Therefore, human PDL cells were cultured in composite scaffolds.

The gene expression of BSP and CAP was examined in vitro; the protein expression of ALP and OPN was evaluated in vivo. BSP and OPN are two major non-collagenous proteins of bone and cementum. It was reported that both BSP and OPN were necessary for the initiation of hard tissue mineralization [21]. During hard tissue formation, BSP acts as a crystal nucleator and OPN ensures that only the right crystal is formed. CAP is a collagenous protein that is found in the developing and mature cementum matrix and cementoblasts. It has been suggested that CAP is a marker molecule for cementogenesis [22], and that CAP is related to the development of the cementoblast phenotype. ALP is a membrane-bound enzyme abundant early in bone formation. The increase of ALP levels had been found to correlate with the increase of bone formation histomorphometrically [23]. ALP is widely recognized as an early stage marker of cellular differentiation towards an osteoblast phenotype. Further, ALP also has been involved in cementogenesis [24]. Therefore, we analyzed the effect of composite scaffold on BSP, CAP, ALP, and OPN synthesis, and we found the levels of BSP and CAP gene expression in the HPLCs cultured in composite scaffolds increased compared with those of the control. In vivo, we

found the levels of ALP and OPN protein expression in the HPLCs in composite scaffold were higher than those of the control. These findings suggested that composite scaffold successfully promoted the ability of HPLCs to synthesize genes and proteins associated with bone and cementum formation both in vitro and in vivo.

The ideal goal of clinical therapy in periodontal defects is regeneration of all lost structures. For the realization of regeneration, cell proliferation, migration, and differentiation are necessary. Besides, in treating periodontal disease, it is essential the HPLCs proliferate faster than that of the surrounding supporting tissue cells [25]. Therefore, the regulation of HPLCs proliferation in the periodontium is crucial for periodontal tissue regeneration. In the present study, the proliferative effect of composite scaffolds on HPLCs had been examined in vitro, and the composite scaffolds obviously stimulated the cellular responses when compared with the pure chitosan scaffolds. TCP have been reported to support the differentiation of relevant cells [10] ,and the results of the present study are in agreement with this report. BSP, CAP, ALP, and OPN are expressed by differentiated osteoblasts or cementoblasts, so the high levels of expression of these genes and proteins in the HPLCs cultured in composite scaffolds suggested that composite scaffolds significantly promoted the differentiation of HPLCs towards osteoblast and cementoblast phenotypes. The addition of TCP might increase the proliferation and differentiation of HPLCs through these approaches: (1) The TCP could improve the initial attachment of the cells, as has been reported [10]. The initial cell attachment directly affects further cellular responses, such as movement, proliferation, and phenotype expression of cells through the internal signal transduction [26]. At the same time, addition of the TCP might increase the scaffold surface area. Therefore, the improved cell attachment on the composites affected further proliferation level. (2) The biocompatibility of the scaffold increased because of the addition of TCP. The TCP was a suitable material for constructing artificial substitutes for damaged tissues and organs, and it promoted cell adhesion and proliferation [10]. (3) The TCP powders were dispersed homogeneously on the surfaces of the solid walls of the pores, which are expected to dissolve slowly in physiological media and increase the concentrations of the Ca and P ions [13]. The increase of the concentrations of the Ca and P ions may play an important role in regulation of the proliferation and differentiation of HPLCs. For example, inorganic phosphate has been reported to be an important regulator of cementoblast functions including maturation and regulation of matrix mineralization [27].

CLSM and FDA were used to observe the morphology and distribution of HPLCs in β-TCP/chitosan composite scaffolds. This method offers several advantages for observation of cells cultured in scaffolds when compared with SEM. First, FDA (no fluorescence), a 'vital dye', could penetrate through the cell membranes. Then it was hydrolyzed into fluorescein by the viable cells. Therefore, only viable cells could be observed by CLSM. In contrast, SEM could only provide images of dead and fixed cells, which could not reflect the true condition of cells. Second, the preparation of samples with FDA for CLSM is simple, so this method almost provides a real-time observation for cells. Further, CLSM not only provides images of the scaffold surface, but also images of the inner space and it can guarantee the clarity of the images and easy reconstruction of three-dimensional images. In our study, we observed that 2 days after seeding, HPLCs not only spread on the surface of the scaffold, but also migrated into the inner space (120 μm in depth) to form complex three-dimensional network-like cell clusters. Cell–cell junction was also observed in every case. These findings demonstrated that the β-TCP/chitosan composite scaffold provided a good environment for the adhesion, proliferation, migration, and cell–cell interaction of HPLCs.

5 Conclusions

We constructed β-TCP/chitosan composite scaffold by a freeze-drying method, which exhibited a homogeneous three-dimensional microstructure, suitable pore size (120 μm) and high porosity (91.07%). CLSM observation revealed that composite scaffold provided a good environment for the ingrowth of HPLCs. The composite scaffold showed better cytocomaptibility than pure chitosan scaffold. The gene expression of BSP and CAP involved in bone and cementum formation was up-regulated in composite scaffold. After implanted in vivo, the composite scaffold exhibited excellent biocompatibility, biodegradability, and bioactivity. The protein expression of ALP and OPN reflecting the formation of hard tissue was improved in the composite scaffold. In summary, β-TCP/chitosan composite scaffold provided a good environment for the adhesion, proliferation, migration, and differentiation of HPLCs. It also promoted the ability of HPLCs to synthesize genes and proteins associated with bone and cementum formation both in vitro and in vivo. This study demonstrated the potential of β-TCP/chitosan composite scaffold as a good candidate in periodontal tissue engineering.

Acknowledgment This study was supported by Grant No. 30772445 from the Natural Science Foundation of China.

References

1. Schroder NW, Meister D, Wolff V, Christan C, Kaner D, Haban V, et al. Chronic periodontal disease is associated with

singlenucleotidepolymorphisms of the human TLR-4 gene. Genes Immun. 2005;6:448–51.
2. Giannopoulou C, Cimasoni G. Functional characteristics of gingival and periodontal ligament fibroblasts. J Dent Res. 1996;75: 895–902.
3. Wang LH, Greenwell H, Fiorellini J, Giannobile W, Offenbacher S, Salkin L, et al. Periodontal regeneration. J Periodontol. 2005; 76:1601–22.
4. Nakahara T, Nakamura T, Kobayashi E, Kuremoto K, Matsuno T, Tabata Y, et al. In situ tissue engineering of periodontal tissues by seeding with periodontal ligament-derived cells. Tissue Eng. 2004;10:537–44.
5. Hubbell JA. Biomaterials in tissue engineering. Biotechnology (NY). 1995;13:565–76.
6. Miyazaki S, Ishii K, Nadai T. The use of chitin and chitosan as drug carriers. Chem Pharm Bull. 1981;29:3067–9.
7. Madihally SV, Matthew HW. Porous chitosan scaffolds for tissue engineering. Biomaterials. 1999;20:1133–42.
8. Hammerle CH, Olah AJ, Schid J, Fluckiger L, Gogolewski S, Winkler JR, et al. The biological effect of natural bone mineral on bone neoformation on the rabbit skull. Clin Oral Implants Res. 1997;8:198–207.
9. Hench LL. Bioceramics: from concept to clinic. J Am Ceram Soc. 1991;74:1487–510.
10. Brown S, Clarke I, Williams P. Bioceramics 14: proceedings of the 14th international symposium on ceramics in medicine. California: Palm Springs; 2001.
11. Zhang K, Wang Y, Hillmayer MA, Francis LF. Processing a properties of porous poly (L-lactide)/bioactive glass composites. Biomaterials. 2004;25:2450–89.
12. Zhang Z, Chen H, Li CK. The methods of alkaline phosphatase staining. In: Zhang Z, Chen H, editors. The manual of pathological staining technique. Liaoning: Liaoning scientific and technical publishing house; 1988. p. 254–5.
13. Zhang Y, Zhang M. Syhthesis and characterization of macroporous chitosan/calcium phoshpate composite scaffolds for tissue engineering. J Biomed Mater Res. 2001;55:304–12.
14. Somerman MJ, Young MF, Foster RA, Moehring JM, Imm G, Sauk JJ. Characteristics of human periodontal ligament cells in vitro. Arch Oral Biol. 1990;35:241–7.
15. Ma PX, Langer R. Fabrication of biodegradable polymer foams for cell transplantation and tissue engineering. In: Yarmush M, Morgan J, editors. Tissue engineering methods and protocols. Totowa NJ: Humana Press Inc; 1999. p. 47–56.
16. Finn AR, Bell HW, Brammer AJ. Interpositional "grafting" with autogenous bone and coralline hydroxyapatite. J Maxillofac Surg. 1980;8:217–27.
17. Nehrer S, Breinan HA, Ramappa A, Young G, Shorkroff S, Louie LK, et al. Matrix collagen type and pore size influence behavior of seeded canine chondrocytes. Biomaterials. 1997;18:769–76.
18. O'Brien FJ, Harley BA, Yannas IV, Gibson LJ. The effect of pore size on cell adhesion in collagen-GAG scaffolds. Biomaterials. 2005;26:433–41.
19. Taba M, Jin Q, Sugai VJ, Giannobile VW. Current concepts in periodontal bioengineering. Orthod Craniofac Res. 2005;8:292–302.
20. Seo BM, Miura M, Gronthos S, Bartold PM, Batouli S, Brahim J, et al. Investigation of multipotent postnatal stem cells from human periodontal ligament. Lancet. 2004;364:149–55.
21. Roach HI. Why does bone matrix contain non-collagenous proteins? The possible roles of osteocalcin, osteonectin, osteopontin and bone sialoprotein in bone mineralisation and resorption. Cell Biol Int. 1994;18:617–28.
22. Arzate H, Olson SW, Page RC, Gown AM, Narayanan AS. Production of a monoclonal antibody to an attachment protein derived from human cementum. FASEB J. 1992;6:2990–5.
23. Franceschi RT, Iyer BS. Relationship between collagen synthesis and expression of the osteoblast phenotype in MC3T3-E1 cells. J Bone Miner Res. 1992;7:235–46.
24. Miao D, Scutt A. Histochemical localization of alkaline phosphatase activity in decalcified bone and cartilage. J Histochem Cytochem. 2002;50:333–40.
25. Sculean A, Windisch P, Chiantella GC, Donos N, Brecx M, Reich E. Treatment of intrabony defects with enamel matrix proteins and Guided tissue regeneration. A prospective controlled clinical study. J Clin Periodontol. 2001;28:397–403.
26. Anselme K. Osteoblast adhesion on biomaterials. Biomaterials. 2000;21:667–81.
27. Foster BL, Nociti FH Jr, Swanson EC, Matsa-Dunn D, Berry JE, Cupp CJ, et al. Regulation of cementoblast gene expression by inorganic phosphate in vitro. Calcif Tissue Int. 2006;78:103–12.